Utilization of alkali-activated olivine in soil stabilization and the effect of carbonation on unconfined compressive strength and microstructure

Mohammad Hamed Fasihnikoutalab[1], Afshin Asadi[2], Cise Unluer[3], Bujang Kim Huat[4], Richard J Ball[5], Shahram Pourakbar[6]

[1]PhD, Department of Civil Engineering, University Putra Malaysia, 43400 UPM, Serdang, Selangor, Malaysia (corresponding author) Email: hfasih@gmail.com

[2]Research Fellow, Housing Research Centre, Department of Civil Engineering, University Putra Malaysia, 43400 UPM, Serdang, Selangor, Malaysia,

[3]Lecturer, School of Civil & Environmental Engineering, Nanyang Technological University, 50 Nanyang Avenue, Singapore 639798, Singapore,

[4]Professor, Department of Civil Engineering, University Putra Malaysia, 43400 UPM, Serdang, Selangor, Malaysia,

[5]Reader in Materials, BRE Centre for Innovative Construction Materials, Department of Architecture and Civil Engineering, University of Bath, Bath, BA2 7AY, UK.

[6]PhD, Department of Civil Engineering, University Putra Malaysia, 43400 UPM, Serdang, Selangor, Malaysia.

Abstract. This paper reports for the first time the stabilisation of soil using olivine and the application of novel techniques utilising alkaline activation and carbonation. A rigorous study addressing the effect carbon dioxide pressure and alkali concentration (10 M sodium hydroxide soil additions from 5 to 20%) was assessed between 7 and 90 days. Microstructural and compositional changes were evaluated using microscopic, spectroscopic and diffraction techniques. Results demonstrate the advantages of using olivine in the presence of NaOH and the associated increases in soil shear strength of up to 40% over 90 days. Samples subjected to carbonation for a further 7 days led to additional increases in soil strength of up to 60%. Microstructural investigations before and after carbonation attributed the strength development to the formation of $Mg(OH)_2$, hydrated magnesium carbonates and M-S-H, A-S-H gel phases. The impact of this work is far reaching and provides a new soil stabilisation approach. Key advantages include significant improvements in soil strength with a lower carbon footprint compared to lime or cement stabilisation.

Keywords: *Olivine, Alkaline activation, Soil stabilization, Carbonation, Microstructure analysis*

INTRODUCTION

Cement is widely used as a binder in soil stabilization for ground improvement (Farouk & Shahien, 2013; Horpibulsuk, 2012). However, one of the main problems with this approach is the release of significant quantities of CO_2 into the atmosphere and high energy utilization during cement production (Y. Yi et al., 2013). Binders based on alkali-activated materials have received a significant interest due to their improved sustainability (P. Duxson, Fernández-Jiménez, et al., 2007; Pourakbar, Huat, Fasihnikoutalab, & Asadi, 2015). The alkali activation process attributed to activators such as sodium hydroxide (NaOH) or potassium hydroxide (KOH) involves the dissolution and subsequent condensation of aluminosilicate materials, which are mostly industrial wastes and by-products (Duxson and Provis 2008). However, the co-existence of geopolymeric gel and an alkaline metal silicate hydrate such as calcium silicate hydrate (C-S-H) has also been reported. In the presence of adequate calcium within the geopolymeric structure, C–(A)–S–H or (C,N)– A–S–H-based cementitious materials may form instead (Guo et al. 2010; Reig et al. 2014). A few studies have investigated the effectiveness of alkali-activated fly ash as silica and alumina amorphous sources for soil stabilisation (Cristelo et al. 2011, 2012; , 2013). Zhang et al. (2013) recently investigated the feasibility of using metakaolin as an alkali-activated soil stabiliser. Pourakbar et al. (2015) reported the use of palm oil fuel ash as a source binder, demonstrating the successful use of alkali-activated binders in soil stabilisation. These studies were conducted by mixing the industrial waste materials and by-products with soft soils in the presence of NaOH and a silica-rich source such as sodium silicate as the alkali activator. The results demonstrate the effectiveness of alkali-activated binders for soil stabilization. A variety of source materials such as kaolin (Slaty et al. 2013), metakaolin (Wang et al. 2005), fly ash (Zhang et al. 2014b), GGBS (Yusuf et al. 2014) and palm oil fuel ash (Liu et al. 2014) are currently being considered for this purpose. However most binders require pre-treatments such as calcination and grinding to increase the reactivity of the Al and Si phases present (Duxson et al. 2007b; Li et al. 2010; Weng and Sagoe-Crentsil 2007). In the case of processes such as calcination, high temperatures are required with associated impact on energy usage and CO_2 emissions.

This paper focuses on the use of olivine (Mg_2SiO_4) to provide a more sustainable approach for the preparation of alkali activated binders to be used in soil stabilization. Olivine presents a sustainable alternative as its sources are widely available globally (Target map 2012) and the financial and environmental costs of olivine processing (mining, milling and transport) are far less than those of cement/lime (Schuiling and Praagman 2011). Its weak nesosilicate structure and the absence of strong Si-O-Si bonds leaves olivine susceptible to dissolution and subsequent chemical reaction (Schuiling 2001, 2013). Its high SiO_2 and alkaline metal content makes this natural resource a good candidate for alkali activation.

Olivine has a high affinity for the adsorption of CO_2 in the presence of water, as shown in Equations 1 and 2 (Dufaud et al. 2009, Fasihnikoutalab et al. 2015c). Similarly, the hydration product of MgO, brucite ($Mg(OH)_2$) can carbonate to produce magnesite ($MgCO_3$) or hydrated magnesium carbonates (HMCs) such as nesquehonite ($MgCO_3 \cdot 3H_2O$), dypingite ($(Mg)_5(CO_3)_4(OH)_2 \cdot 5H_2O$), and hydromagnesite ($(Mg)_5(CO_3)_4(OH)_2 \cdot 4H_2O$), as shown in Equations 3 to 5 (Y. Yi et al., 2013; Unluer & Al-Tabbaa, 2013). The carbonation of olivine has been reported to improve the unconfined compressive strength (UCS) and ultimate bearing capacity of soil (Fasihnikoutalab, et al., 2015a; 2015b).

$$Mg_2SiO_4 + 4H_2O \rightarrow 2Mg(OH)_2 + H_4SiO_4 \quad (1)$$

$$Mg(OH)_2 + CO_2 \rightarrow MgCO_3 + H_2O \quad (2)$$

$$Mg(OH)_2 + CO_2 + 2H_2O \rightarrow MgCO_3 \cdot 3H_2O \quad (3)$$

$$5Mg(OH)_2 + 4CO_2 + H_2O \rightarrow (Mg)_5(CO_3)_4(OH)_2 \cdot 5H_2O \quad (4)$$

$$5Mg(OH)_2 + 4CO_2 \rightarrow (Mg)_5(CO_3)_4(OH)_2 \cdot 4H_2O \quad (5)$$

Blencoe and Palmer (2004) reported the use of a strong base such as sodium hydroxide (NaOH) to break the chemical bond between MgO and SiO_2. This leads to the production of $Mg(OH)_2$ and Na_2SiO_3, as shown in Equation 6 (Zhao and Zhai 2013). An intermediate step can involve the reaction of CO_2 with NaOH to improve the CO_2 adsorption potential. The reaction products are alkali-metal carbonate (Na_2CO_3) or bicarbonate ($NaHCO_3$) and silica in either a gelatinous or solid form, as shown in Equations 6-8 (Blencoe and Palmer 2004).

$$Mg_2SiO_4 + 2NaOH + H_2O \rightarrow 2Mg(OH)_2 + Na_2SiO_3 \quad (6)$$

$$Na_2SiO_3 + 2CO_2 + H_2O \rightarrow 2NaHCO_3 + SiO_2 \quad (7)$$

$$2Mg(OH)_2 + 2NaHCO_3 \rightarrow 2MgCO_3 + 2NaOH + 2H_2O \quad (8)$$

Due to its role as an effective source of MgO and SiO_2 with weak chemical bonds, olivine can be an ideal candidate for soil stabilization after being subjected to alkali activation and carbonation. Moreover, one of the great advantages of stabilising soil using olivine as a binder in the presence of a strong alkali is that pre-treatments which are often energy intensive are not required. This process can be induced by the introduction of NaOH to increase the carbonation potential of olivine. This study aims to explore the carbonation of alkali-activated olivine used in soil stabilization. The behaviour of olivine treated soil was examined through UCS measurements before and after carbonation treatment. The composition and microstructural development of activated olivine treated soils were examined using scanning electron microscopy (SEM), energy-dispersive X-ray spectroscopy (EDX), X-ray diffraction (XRD) and Fourier transform infrared spectroscopy (FTIR) before and after carbonation.

MATERIALS AND METHODOLOGY

The soil used in this research contained 60% silt, 30% clay and 10% sand with a mean particle size (D_{50}) of 11.759 μm and a specific surface area (SSA) of 1.04 m^2/g. Table 1 shows the physicochemical and engineering properties of soil as-received and soil treated with different percentages of olivine. Based on the Unified Soil Classification System (USCS), the soil is classified highly plastic (CH).

Table1. Physicochemical and engineering properties of soil and olivine treated soil

Olivine was sourced from MAHA chemical company in Malaysia. The chemical composition of olivine obtained using XRF is listed in Table 2. The PSD of the olivine given in Figure 1 shows the D_{50} and SSA of olivine as 2.24 μm and 6.07 m^2/g, respectively.

Fig.1. Particle size distribution of olivine

NaOH was selected as a source of Na^+ and OH^- for the alkali activation process. The NaOH used in this study was supplied in a flake form by R&M Chemicals in Malaysia.

Table2. Chemical composition of olivine determined by XRF

Methodology

Mix composition and sample preparation

The compositions of the various mixes of soil, olivine, NaOH and water prepared during this study are listed in Table 3. The concentration of NaOH was fixed at 10M for all samples in line with the findings of previous studies (Cristelo et al. 2011; Cristelo et al. 2012b).

To prepare the samples, the alkali activator was dissolved in distilled water at the predetermined concentration (10M). The compaction test was conducted to achieve the optimum water content (OWC) and maximum dry density (MDD) of the alkaline activated soil and alkaline activated olivine treated soil mixtures (British Standard 2003a). Following drying for 24 hours the soil was mixed with 5, 10, 15 and 20% olivine and 10M NaOH, a pure soil was also tested as a reference. Specimens were placed in cylindrical moulds onto which consistent moderate compaction was applied, and extruded. All specimens were prepared for UCS before and after carbonation at OWC and MDD. Immediately after extrusion, mix C_{PT}A20 was subjected to carbonation under different CO_2 pressures and durations (Table 3). The rest of specimens (A5, A10, A15 and A20) were wrapped in polythene covers to avoid water loss and cured under ambient conditions in different curing regimes prior to UCS testing (Table 3).

Carbonation

A triaxial reactor was used to carbonate mix C_{PT}A20 by allowing pressurized gaseous CO_2 (100 and 200 kPa) to permeate through the olivine treated soil for 12, 24, 48 and 168 hours. Immediately after moulding, samples were subjected to carbonation under a confining pressure of 400 kPa during which CO_2 permeated upwards. The CO_2 saturation level was detected by the outflow tube placed underwater

Table 3. Mix compositions prepared under this study

UCS

The UCS test was performed on carbonated (at 12, 24, 48 and 168 hours) and uncarbonated (at 7, 14, 28, and 90 days) samples immediately after carbonation/curing according to BS 1924: Part 7 (British Standard 2003b). The equipment used for this purpose was an Instron 3382, with 100 kN capacity.

Microstructural analysis

Samples were examined before and after carbonation by an SEM JSM 5700 coupled with an EDX spectrometer. Samples were sputter coated with gold before analysis to increase the electrical conductivity of the surface and reduce charging. Crystalline phases were investigated using a Philips X-Ray diffractometer XRD between 3-50° 2θ. The composition of samples before and after carbonation was investigated under FTIR via a Perkin Elmer Paragon 100 Spectrometer within a spectra of 4000-500 cm^{-1}.

RESULTS

UCS

Figure 2 shows the stress-strain behaviour of soil (S), alkali-activated soil (AS) and alkaliactivated soil with different percentages of olivine (A5, A10, A15, and A20) after 7, 14, 28 and 90 days of curing. Untreated soil specimens (S) showed a ductile behaviour with the strength of 103.4 kPa at a failure strain of around 1.8%. Alkali activation increased the strength of soil to 240.9, 263.0, 370.3 and 521.7 kPa at 7, 14, 28, and 90 days, respectively. The slight increase in the strength of soil specimens observed in the presence of NaOH was attributed to the role of NaOH in promoting the dissolution of Si and Al within soil (Cristelo et al. 2011). The increase in the strength of AS was not significant due to the low reactivity of Si and Al. A progressive increase in strength was observed when different amounts of olivine were used. The strength of samples increased with olivine content (0 to 20%) and curing time (7 to 90 days). A20 achieved the highest strength within all alkali treated soil samples, resulting in 850.3, 1016.9, 1210.5 and 3964.8 kPa at 7, 14, 28 and 90 days, respectively.

Fig.2. UCS of alkaline activated olivine treated soil at: a) 7, b) 14, c) 28 and d) 90 days

Figure 3 shows the variation of UCS with the Na/olivine mass ratio ranging between 0.30 and 1.36 over a 90-day period. Strength generally increased as the Na/olivine ratio decreased. The maximum UCS was obtained at the lowest Na/olivine ratio of 0.30 for all curing periods. This ratio could set a guideline for the design of compositions with improved mechanical performance. These findings are consistent with previous literature, which report an increase in strength with a reduction in activator/source binder ratios (Cristelo et al. 2011, 2012b; Duxson et al. 2007b). This might be explained using the dry unit weight-liquid content relationship theory for soil stabilization. As shown in Table 3, olivine additions to the treated soil in the presence of 10M NaOH decreased the OWC and increased the MDD. However, the highest MDD and the lowest OWC were obtained when the Na/olivine ratio was at a minimum (i.e. 0.3).

Fig.3. Influence of Na/olivine weight ratio on strength development at 7, 14, 28 and 90 days

Figure 4 shows the stress-strain behaviour of alkali-activated soil with 20% olivine (A20) after 90 days of curing and soil treated with 20% olivine in the presence of 10M NaOH subjected to carbonation at 100 and 200 kPa for up to 168 hours. An increase in the UCS was observed with an increase in the carbonation pressure and duration. Strength rapidly increased when the CO_2 pressure and duration increased from 100 to 200 kPa and 12 to 168 hours, respectively. When compared to uncarbonated alkali-activated 20% olivine treated soils at 90 days, the corresponding samples subjected to carbonation ($C_{(200,168)}A20$) achieved higher strengths. The results show that

olivine is a promising candidate for soil stabilization as alkali activated olivine treated soils were sufficiently carbonated within a few days to achieve strengths required for ground improvement.

Fig.4. UCS of carbonated alkaline activated olivine treated soil subjected to carbonation for 12, 24, 48 and 168 hours at pressures of 100 and 200 kPa.

SEM characterization

Figure 5(a) shows that the microstructure of soil consists of clusters of particles, whereas the irregular shape of olivine particles are seen in Figure 5(b). Figure 5(c) illustrates the olivine treated soil after 90 days of curing. A comparison of Figures 5(a) and (c) reveals how the olivine fills the pores of the soil as a result of its delayed hydration and pozzolanic reaction within the soil. Figures 5(d)-(f) show the microstructure of 20% olivine treated soil in the presence of 10M of NaOH after 90 days curing. SEM images demonstrate a compact morphology without any major discontinuities, which is consistent with the mechanical properties observed. The presence of a new amorphous phase is evident in Figures 5(d)-(f), which reveal the formation of a gelatinous structure and crystals on the surface of the samples and around the particles of the starting material. SEM images of samples subjected to carbonation at a CO_2 pressure of 200 kPa for 12, 24, 48 and 168 hours shown in Figures 6(a)-(d) demonstrate a denser and more homogenous microstructure with an increase in carbonation duration.

Fig.5. SEM images of: a) Soil, b) olivine, c) olivine treated soil and d-f) alkaline activated olivine treated soil after 90 days curing

Fig.6. SEM images of: a) $C_{(200,12)}A20$, b) $C_{(200,24)}A20$, c) $C_{(200,48)}A20$ and d) $C_{(200,168)}A20$

EDX characterization

Table 4 shows the Si/Al and Na/Al molar ratios calculated from EDX data for samples cured for 90 days or carbonated under a CO_2 pressure of 200kPa for different periods. An increase in the strength of soils was observed with an increase in the Si/Al and Na/Al ratios after 90 days, which was in line with previous studies demonstrating higher strengths at Si/Al ratios between 1.15 and 2.15 (Cristelo et al., 2013; P. Duxson et al., 2007). Carbonated samples revealed higher Si/Al and Na/Al ratios (1.49 and 0.77) than uncarbonated samples (1.24 and 0.32). This corresponded to a larger degree of geopolymerization attributed to the higher Na/Al ratio. Na^+ cations also played a role in balancing the net negative charge of Al^{3+} resulting from the Al:O coordination (Cristelo, Glendinning, Miranda, et al., 2012; M. Zhang et al., 2014).

Table 4. Molar ratios calculated from EDX data and UCS of alkaline activated olivine treated soil

FTIR characterization

Figure 7 shows the FTIR of four samples within the range of 650-4000 cm^{-1} containing 5, 10, 15 and 20% olivine treated soil after 90 days. The band at 3693 cm^{-1}, present in all samples, is associated to O-H stretching within brucite. Previous studies report the characteristic Mg–OH stretch of phyllosilicates near 3690 cm^{-1} and a weak stretch in the Mg–OH region (Lee and Van

Deventer 2002a). Bands correspond to O–H stretching in the range of 3394-3401 cm^{-1} support H–bonds in all samples, referring to the presence of water even after 90 days of curing. This could explain the greater strengths observed at longer curing times in terms of full reaction.

However, very weak absorptions near 1220 cm^{-1} attributed to Si–O vibrations may be an indication of silica polymerisation in M-S-H gels. The formation of an amorphous aluminosilicate gel as a result of dissolution of olivine with the introduction of NaOH was evident at 1080-1100 and 980-1040 cm^{-1} related to Si-O bond and asymmetric stretching vibrations of Si-O/Al-O bonds, respectively (Criado et al. (2005). Bands at 914, 790-730 and 680-650 cm^{-1} were connected to Al-OH, Al-O bond stretching and Si-O vibration stretching, respectively (Abdul Rahim et al. (2014).

Fig.7. FTIR of alkaline activated olivine treated soil at different curing time

Figure 8 shows the FTIR characterization of 20% of olivine treated soil after carbonation at a CO_2 pressure of 200 kPa at different durations of 12, 48 and 168 hours. The peaks correspond to the presence of an amorphous aluminosilicate gel. Bands at 950 and 797 cm^{-1} were attributed to the asymmetric and symmetric stretching vibration of Si-O-Si and Al-O-Si bonds, indicating the extent of carbonation within these samples. The changes at 1220 cm^{-1} after carbonation refer to the changes in the chain structure of M-S-H, indicating the decomposition of M-S-H by carbonation and a higher degree of polymerization and lengthening of silicates within the remaining gel. These results confirm the findings of previous studies on the role of carbonation in the geopolymerization of slag. It is therefore possible that Mg^{2+} plays a similar role as Ca^{2+} when it is present within the geopolymeric gel phase (Lee and Van Deventer 2002a; b).

The strong peaks shown between 1410-1570 cm^{-1} in Figure 8 are attributed to C-O vibrations from the adsorption of CO_2 and formation of carbonates in solution, which might be in close association with Na^+ or Mg^{2+} cations (Abdul Rahim et al. (2014). The bands between 1450-1650 cm^{-1} related to the asymmetric stretching of CO_3^{-2} gained intensity as the carbonation duration increased due to the formation of $MgCO_3$ and $NaHCO_3$.

Bands at 3350 and 1647 cm^{-1} were related to O-H and H-O-H stretching and bending vibrations. Bands 3600-3000 cm^{-1} were correlated to–OH stretching and H-O-H bending of vibrations in water molecules. The decrease observed in the vibrations corresponding to the O–H after carbonation is in agreement with previous findings (Song et al. 2014). This is most obvious as the carbonation duration increased from 48 to 168 hours, leading to the disappearance of the 3690 cm^{-1} band originally attributed to brucite.

Fig.8. FTIR of carbonated alkaline activated olivine treated soil at 200 kPa pressure after 12, 48, 168 hours

XRD characterization

Figure 9 shows the XRD of 20% of olivine treated soil after 90 days of ambient curing. Peaks of brucite, quartz, serpentine, kaolinite, mullite, sodium silicate (Na_2SiO_3) and Mg peak are detected as a result of olivine dissolution through the sodium hydroxide in soil. Peaks of quartz (SiO_2) (9, 24, 26, 28, 39 and 45°), brucite (18, 21, 36 and 48°) and sodium silicate (30 and 35°) were detected throughout the patterns (Komljenović et al. 2010; Yi et al. 2013c).

Fig.9. XRD of A20 after 90 days curing time (B:brucite, K:kaolinite, Mg:MgO, M:mullite, S:serpentine, SS:sodium silicate, Q:quartz)

Figure 10 (a-c) shows the XRD analysis of 20% olivine treated soil after 12, 48 and 168 hours carbonation under 200 kPa. Increasing carbonation periods led to a decrease in the brucite and magnesium peaks, whereas and nesquehonite peaks increased as result of the carbonation process. The sodium silicate peak decreased due to its reaction with CO_2 and brucite as shown in Equation 7.

Fig.10.XRD of a) $C_{(12,200)}$A20, b) $C_{(48,200)}$A20, c) $C_{(168,200)}$A20 (B:brucite, H/D:hydromagnesite/dypingite, Mg:MgO, N:nesquehonite, Q:quartz, S:serpentine, SS:sodium silicate)

DISCUSSIONS

When olivine is mixed with NaOH within a soil mix, it breaks the chemical bond between MgO and SiO_2 and leaches the silicon from amorphous phases within olivine grains as described by Equation 6. As a result of this leaching, $Mg(OH)_2$ and Na_2SiO_3 are produced as confirmed by FTIR and XRD results (Figures 7 and 9). The Na_2SiO_3 produced from the reaction of olivine with NaOH in the presence of water can also act as an activator. Previous studies report the use of activators such as NaOH and Na_2SiO_3 to promote the dissolution of phases and subsequent alkaline activation (Abdul Rahim et al. 2014, Phoo-ngernkham et al. 2015). The presence of NaOH and Na_2SiO_3 could result in the leaching of the Si and Al in the amorphous phases of soil, producing an alumina-silica-hydrate (A-S-H) gel.

The addition of calcium (Ca) was shown to have a positive effect on the mechanical properties of alkali activated binders (Temuujin et al. 2009). Olivine is rich in MgO (48%), from which the release of Mg ions may exhibit a similar behaviour to Ca ions due to their similar charge. Therefore, besides Si and Al, Mg ions may play a significant role in crystal growth. In the presence of an alkali activator, Mg ions could provide additional nucleation sites for the precipitation of dissolved species and contribute to the formation of magnesium silicate hydrate (M-S-H) gel (Salih et al. 2014; Yip et al. 2008).

The strength development of the alkali-activated soil with different percentages of olivine (Figure 3) could be attributed to (i) formation of $Mg(OH)_2$ which is an expansive process filling the available pores (Y. Yi et al., 2013; Zhu, Ye, Liu, & Yang, 2013); and (ii) formation of M–S– H and A-S-H gels. As a result, a compact morphology was observed, which is consistent with the mechanical properties.

According to the FTIR and XRD results after carbonation, reaction of NaOH with olivine leads to the formation of Na_2SiO_3, which subsequently reacts with CO_2 dissolved in water, forming $NaHCO_3$ and SiO_2. $Mg(OH)_2$ then reacts with $NaHCO_3$ and forms $MgCO_3$ (Equation 8). This is attributed to the ability of HMCs (nesquehonite, dypingite and hydromagnesite) to form wellramified networks of massive crystals with a very effective binding ability (Y. Yi et al., 2013). This consequently led to a soil with a denser and more homogenous microstructure (Figure 6), transforming into increased strength gain. Another advantage of using olivine in the presence of

NaOH is the formation of double carbonate eitelite ($Na_2Mg(CO_3)_2$) from the reaction of $Mg(OH)_2$ and Na_2CO_3 at elevated CO_2 levels. Eitelite contains CO_2 in the form of $MgCO_3$ which enables the sequestration of twice the amount of CO_2 per ton of mined Mg rich rock (Blencoe and Palmer 2004).

The study confirms olivine is promising as a sustainable stabilisation binder through the adsorption of CO_2. Results show that olivine can achieve high strengths through the absorption of greater quantities of CO_2 in the presence of NaOH with associated environmental benefits. In addition the cost of olivine, when compared to other binders used for soil stabilization such as cement and lime, highlight the important economic benefits of using olivine for soil stabilization.

Furthermore this research indicates that carbonation of alkali-activated olivine-treated soils in field trials may be achieved by adopting mass carbonation stabilisation or deep mixing carbonation methods (Cai et al. 2015, Yi et al. 2013b).

CONCLUSIONS

This study for the first time investigated the role of alkali activated olivine treated soil before and after carbonation. The results demonstrate that 20% olivine is an optimal quantity for use as a source binder in carbonating alkali activated treated soil. The strength of olivine treated soil in the presence of NaOH increased with olivine content and curing time, reaching a value up to 40% higher than untreated soil. The carbonation of alkali activated olivine treated soil at a CO_2 pressure of 200 kPa increased the strength of soil up to 60% greater than the untreated soil and 1.5% greater than the alkali activated olivine treated soil after 90 days of curing. Microstructural analyses confirmed the strength development of the alkali activated olivine treated soil, which was attributed to the formation of $Mg(OH)_2$, M–S–H and A-S-H gels. Further strength development was attributed to carbonation with the formation of HMCs, nesquehonite and hydromagnesite/dypingite. The dissolution mechanism of olivine before and after carbonation and the influence of Si/Al and Na/Al ratios of alkali activated systems also led to an increase in strength as confirmed by EDX results and mechanical testing. The formation of the final gel was also confirmed by FTIR results. This study has identified the successful use of olivine in the treatment of soil in the presence of an alkali activator. The results have also demonstrated that carbonation can rapidly increase the strength of soil.

Acknowledgment

The authors sincerely thanks to the University Putra Malaysia and Fundamental Research Grant Scheme (FRGS/1/2015/TK01/UPM/01/2) entitled "sustainable soil stabilization by olivine and its mechanisms" funded by Ministry of Higher Education in Malaysia (Vote Number: 5524745) for financial support of this research. Moreover, sincere thanks are due to Prof. emeritus Dr. R.D. Schuiling from the Netherlands who sparked the idea of using olivine for soil improvement and stabilization and shared some particularly fruitful discussions with us.

References:

Abdul Rahim, R. H., Azizli, K. A., Man, Z., Rahmiati, T., and Nuruddin, M. F. (2014). "Effect of Sodium Hydroxide Concentration on the Mechanical property of Non Sodium Silicate Fly Ash Based Geopolymer." *Journal of Applied Sciences*, 14(23), 3381–3384.

Blencoe, J., and Palmer, D. (2004). "Carbonation of metal silicates for long-term CO2 sequestration." *US Paten*, USA.
British Standard, I. (2003a). "British Standard Methods of test for Soils for civil engineering purposes. Part 4: Compaction-related tests. BS 1377-4: 1990." *British Standard*, 1–53.
British Standard, I. (2003b). "British Standard Methods of test for Soils for civil engineering purposes. Part 7: Shear strength tests (total stress). BS 1377-7:1990."
Cai, G.-H., Du, Y.-J., Liu, S. L., and Singh, D. . (2015). "Physical Properties, Electrical Resistivity and Strength Characteristics of Carbonated Silty Soil Admixed with Reactive Magnesia." *Canadian Geotechnical Journal*, 52(999), 1–15.
Criado, M., Palomo, a, and Fernandezjimenez, a. (2005). "Alkali activation of fly ashes. Part 1: Effect of curing conditions on the carbonation of the reaction products." *Fuel*, 84(16), 2048–2054.
Cristelo, N., Glendinning, S., Fernandes, L., and Pinto, A. T. (2012a). "Effect of calcium content on soil stabilisation with alkaline activation." *Construction and Building Materials*, Elsevier Ltd, 29, 167–174.
Cristelo, N., Glendinning, S., Fernandes, L., and Pinto, A. T. (2013). "Effects of alkalineactivated fly ash and Portland cement on soft soil stabilisation." *Acta Geotechnica*, 8(4), 395–405.
Cristelo, N., Glendinning, S., Miranda, T., Oliveira, D., and Silva, R. (2012b). "Soil stabilisation using alkaline activation of fly ash for self compacting rammed earth construction." *Construction and Building Materials*, Elsevier Ltd, 36, 727–735.
Cristelo, N., Glendinning, S., and Pinto, A. T. (2011). "Deep soft soil improvement by alkaline activation." *Proceedings of the ICE - Ground Improvement*, 164(1), 1–10.
Dufaud, F., Martinez, I., and Shilobreeva, S. (2009). "Experimental study of Mg-rich silicates carbonation at 400 and 500 °C and 1 kbar." *Chemical Geology*, Elsevier B.V., 265(1-2), 79–87.
Duxson, P., Fernández-Jiménez, A., Provis, J. L., Lukey, G. C., Palomo, A., and Deventer, J. S. J. (2007a). "Geopolymer technology: the current state of the art." *Journal of Materials Science*, 42(9), 2917–2933.
Duxson, P., Mallicoat, S. W., Lukey, G. C., Kriven, W. M., and van Deventer, J. S. J. (2007b). "The effect of alkali and Si/Al ratio on the development of mechanical properties of metakaolin-based geopolymers." *Colloids and Surfaces A: Physicochemical and Engineering Aspects*, 292(1), 8–20.
Duxson, P., and Provis, J. L. (2008). "Designing precursors for geopolymer cements." *Journal of the American Ceramic Society*, 91(12), 3864–3869.
Farouk, A., and Shahien, M. M. (2013). "Ground improvement using soil–cement columns: Experimental investigation." *Alexandria Engineering Journal*, Faculty of Engineering, Alexandria University, 52(4), 733–740.
Fasihnikoutalab, M. H., Asadi, A., Bujang, K. H., Ball, R. J., Pourakbar, S., and Parminder, S. (2015a). "Utilization of carbonating olivine for soil stabilization." *Environmental Geotechnics*, (In press).
Fasihnikoutalab, M. H., Asadi, A., Bujang, K. H., Westgate, P., Ball, R. J., and Pourakbar, S. (2015b). "Laboratory-Scale Model of Carbon Dioxide Deposition for Soil Stabilization." *Journal of Rock Mechanics and Geotechnical Engineering*, Elsevier Ltd, 8(2), 178–186.
Fasihnikoutalab, M. H., Westgate, P., B.B.K, H., Asadi, A., Ball, R. J., Haslinda, N., and Singh, P. (2015c). "New Insights into Potential Capacity of Olivine in Ground Improvement." *Electronic Journal of Geotechnical Engineering*, 20(8), 2137–2148.
Gartner, E. (2004). "Industrially interesting approaches to 'low-CO2' cements." *Cement and Concrete Research*, 34(9), 1489–1498.

Guo, X., Shi, H., and Dick, W. a. (2010). "Compressive strength and microstructural characteristics of class C fly ash geopolymer." *Cement and Concrete Composites*, Elsevier Ltd, 32(2), 142–147.
Horpibulsuk, S. (2012). "Strength and Microstructure of Cement Stabilized Clay." *INTECH*.
Komljenović, M., Bascarević, Z., and Bradić, V. (2010). "Mechanical and microstructural properties of alkali-activated fly ash geopolymers." *Journal of hazardous materials*, 181(13), 35–42.
Lee, W. K. W., and Van Deventer, J. S. J. (2002a). "The effects of inorganic salt contamination on the strength and durability of geopolymers." *Colloids and Surfaces A: Physicochemical and Engineering Aspects*, 211(2-3), 115–126.
Lee, W. K. W., and Van Deventer, J. S. J. (2002b). "The effect of ionic contaminants on the early-age properties of alkali-activated fly ash-based cements." *Cement and Concrete Research*, 32(4), 577–584.
Li, C., Sun, H., and Li, L. (2010). "A review: The comparison between alkali-activated slag (Si+Ca) and metakaolin (Si+Al) cements." *Cement and Concrete Research*, Elsevier Ltd, 40(9), 1341–1349.
Liu, M. Y. J., Chua, C. P., Alengaram, U. J., and Jumaat, M. Z. (2014). "Utilization of Palm Oil Fuel Ash as Binder in Lightweight Oil Palm Shell Geopolymer Concrete." *Advances in Materials Science and Engineering*, 2014, 1–6.
Phoo-ngernkham, T., Maegawa, A., Mishima, N., Hatanaka, S., and Chindaprasirt, P. (2015). "Effects of sodium hydroxide and sodium silicate solutions on compressive and shear bond strengths of FA–GBFS geopolymer." *Construction and Building Materials*, Elsevier Ltd, 91, 1–8.
Pourakbar, S., Huat, B. B. K., Fasihnikoutalab, M. H., and Asadi, A. (2015). "Soil stabilisation with alkali-activated agro-waste." *Environmental Geotechnics*, 2(6), 359–370.
Reig, L., Soriano, L., Borrachero, M. V., Monzó, J., and Payá, J. (2014). "Influence of the activator concentration and calcium hydroxide addition on the properties of alkali-activated porcelain stoneware." *Construction and Building Materials*, Elsevier Ltd, 63, 214–222.
Ryu, G. S., Lee, Y. B., Koh, K. T., and Chung, Y. S. (2013). "The mechanical properties of fly ash-based geopolymer concrete with alkaline activators." *Construction and Building Materials*, Elsevier Ltd, 47, 409–418.
Salih, M. A., Abang Ali, A. A., and Farzadnia, N. (2014). "Characterization of mechanical and microstructural properties of palm oil fuel ash geopolymer cement paste." *Construction and Building Materials*, Elsevier Ltd, 65, 592–603.
Schuiling, R. (2001). "Olivine, the miracle mineral." *Mineral. Journ. (Ukraine)*, 23(5/6), 81–83.
Schuiling, R. D. (2013). "Olivine: a supergreen fuel." *Energy, Sustainability and Society*, Energy, Sustainability and Society, 3(1), 18.
Schuiling, R., and Praagman, E. (2011). "Olivine Hills: Mineral Water Against Climate Change." *Engineering Earth*, 1–6.
Slaty, F., Khoury, H., Wastiels, J., and Rahier, H. (2013). "Characterization of alkali activated kaolinitic clay." *Applied Clay Science*, Elsevier B.V., 75-76, 120–125.
Song, K.-I., Song, J.-K., Lee, B. Y., and Yang, K.-H. (2014). "Carbonation Characteristics of Alkali-Activated Blast-Furnace Slag Mortar." *Advances in Materials Science and Engineering*, 2014, 1–11.
TARGET MAP. (2012). "Olivine distribution resources." *MapGenia*, <http://www.targetmap.com/viewer.aspx?reportId=24272>.

Temuujin, J., Williams, R. P., and van Riessen, a. (2009). "Effect of mechanical activation of fly ash on the properties of geopolymer cured at ambient temperature." *Journal of Materials Processing Technology*, 209(12-13), 5276–5280.
Turner, L. K., and Collins, F. G. (2013). "Carbon dioxide equivalent (CO2-e) emissions: A comparison between geopolymer and OPC cement concrete." *Construction and Building Materials*, Elsevier Ltd, 43, 125–130.
Unluer, C., and Al-Tabbaa, a. (2013). "Impact of hydrated magnesium carbonate additives on the carbonation of reactive MgO cements." *Cement and Concrete Research*, Elsevier Ltd, 54, 87–97.
Unluer, C., and Al-Tabbaa, A. (2015). "The role of brucite, ground granulated blastfurnace slag, and magnesium silicates in the carbonation and performance of MgO cements." *Construction and Building Materials*, Elsevier Ltd, 94, 629–643.
Wang, H., Li, H., and Yan, F. (2005). "Synthesis and mechanical properties of metakaolinitebased geopolymer." *Colloids and Surfaces A: Physicochemical and Engineering Aspects*, 268(1-3), 1–6.
Wang, S. D., and Scrivener, K. L. (2003). "29Si and 27Al NMR study of alkali-activated slag." *Cement and Concrete Research*, 33, 769–774.
Weng, L., and Sagoe-Crentsil, K. (2007). "Dissolution processes, hydrolysis and condensation reactions during geopolymer synthesis: Part I—Low Si/Al ratio systems." *Advances In Geopolymer Science & Technology. Journal of Materials Science*, 42(9), 2997–3006.
Yi, Y. ., Liska, M., Unluer, C., and Al-Tabbaa, A. (2013a). "Initial investigation into the carbonation of MgO for soil stabilisation." *18th International Conference on Soil Mechanics and Geotechnical Engineering, Paris*, 2641–2644.
Yi, Y., Liska, M., Akinyugha, A., Unluer, C., and Al-Tabbaa, A. (2013b). "Preliminary Laboratory-Scale Model Auger Installation and Testing of Carbonated Soil-MgO Columns." *Geotechnical Testing Journal*, 36(3), 1–10.
Yi, Y., Liska, M., Unluer, C., and Al-Tabbaa, A. (2013c). "Carbonating magnesia for soil stabilization." *Canadian Geotechnical Journal*, 50(8), 899–905.
Yip, C. K., and Van Deventer, J. S. J. (2003). "Microanalysis of calcium silicate hydrate gel formed within a geopolymeric binder." *Journal of Materials Science*, 38(18), 3851–3860.
Yip, C. K., Lukey, G. C., Provis, J. L., and van Deventer, J. S. J. (2008). "Effect of calcium silicate sources on geopolymerisation." *Cement and Concrete Research*, 38, 554–564.
Yusuf, M. O., Megat Johari, M. A., Ahmad, Z. A., and Maslehuddin, M. (2014). "Evolution of alkaline activated ground blast furnace slag–ultrafine palm oil fuel ash based concrete." *Materials & Design*, Elsevier Ltd, 55, 387–393.
Zhang, M., El-Korchi, T., Zhang, G., Liang, J., and Tao, M. (2014a). "Synthesis factors affecting mechanical properties, microstructure, and chemical composition of red mud–fly ash based geopolymers." *Fuel*, Elsevier Ltd, 134, 315–325.
Zhang, M., Guo, H., El-Korchi, T., Zhang, G., and Tao, M. (2013). "Experimental feasibility study of geopolymer as the next-generation soil stabilizer." *Construction and Building Materials*, Elsevier Ltd, 47, 1468–1478.
Zhang, Z., Wang, H., Zhu, Y., Reid, A., Provis, J. L., and Bullen, F. (2014b). "Using fly ash to partially substitute metakaolin in geopolymer synthesis." *Applied Clay Science*, Elsevier B.V., 88-89, 194–201.
Zhao, C., and Zhai, Y. (2013). "Leaching behavior mechanism of Mg_2SiO_4 in high NaOH content system." *The Chinese Journal of Nonferrous Metals*, 23(6), 1764–1768.
Zhu, J., Ye, N., Liu, J., and Yang, J. (2013). "Evaluation on Hydration Reactivity of Reactive

Magnesium Oxide Prepared by Calcining Magnesite at Lower Temperatures." *Industrial & Engineering Chemistry Research*, 52(19), 6430–6437.

Table 1. Physicochemical and engineering properties of soil and olivine treated soil

Water content	
Optimum water content of soil	23.3%
Optimum Water Content of soil + 5% olivine	19.2%
Optimum Water Content of soil + 10% olivine	18.6%
Optimum Water Content of soil + 15% olivine	17.4%
Optimum Water Content of soil + 20% olivine	16.9%
Consistency limits	
Plastic limit	30%
Liquid limit	54%
Plasticity index	24%
Density	2.65
Specific gravity of soil	1.58 g/cm3
Maximum Dry density of soil	1.625 g/cm3
Maximum Dry Density of soil + 5% olivine	1.681 g/cm3
Maximum Dry Density of soil + 10% olivine	1.719 g/cm3
Maximum Dry Density of soil + 15% olivine	1.74 g/cm3
Maximum Dry Density of soil + 20% olivine	10%
Composition	60%
Sand	30
Silt	23.3%
Clay	19.2%

Chemical composition

Fe_2O_3	SiO_2	CaO	Al_2O_3	K_2O	SO_3	MgO	LOI
33.7	28.5	15.8	8.3	4.45	3.75	0.25	5.25

Table 2. Chemical composition of olivine determined by XRF

MgO	SiO_2	Fe_2O_3	Al_2O_3	CaO	LOI
48.3%	40.3%	8.9%	1.4%	-	1.1%

Table 3. Mix compositions prepared under this study

Label	Olivine (%)	NaOH/olivine (Wt)	OWC (%)	MDD (gr/cm^3)	Curing duration
AS	0	0	19.20	1.48	Uncarbonated: 7, 14, 28 and 90 days
A5	5	1.36	17.00	1.52	
A10	10	0.46	16.20	1.58	
A15	15	0.41	15.50	1.65	
A20	20	0.30	15.20	1.69	
C_{PT}-A20	20	0.30	15.20	1.69	Carbonated: 100 and 200 kPa CO_2 pressure for 12, 24, 48 and 168 hours

AS: Alkaline activated treated soilA5, A10, A15 and A20: Alkaline activated olivine treated soil with 5, 10, 15 and 20% olivine

C_{PT}-A20: Carbonated alkaline activated 20% olivine treated soil at a pressure “P” pressure and carbonation time “T”

Table 4. Molar ratios calculated from EDX data and UCS of alkaline activated olivine treated soil

Values	Samples						
	Uncarbonated		(90 days)		Carbonated		
	A5	A10	A15	A20	$C_{(12,200)}A20$	$C_{(48,200)}A20$	$C_{(168,200)}A20$
Si/Al	1.13	1.14	1.18	1.24	1.28	1.40	1.49
Na/Al	0.2	0.23	0.25	0.32	0.36	0.54	0.77
UCS (MPa)	2.05	2.63	3.57	3.95	4.53	5.18	6.02

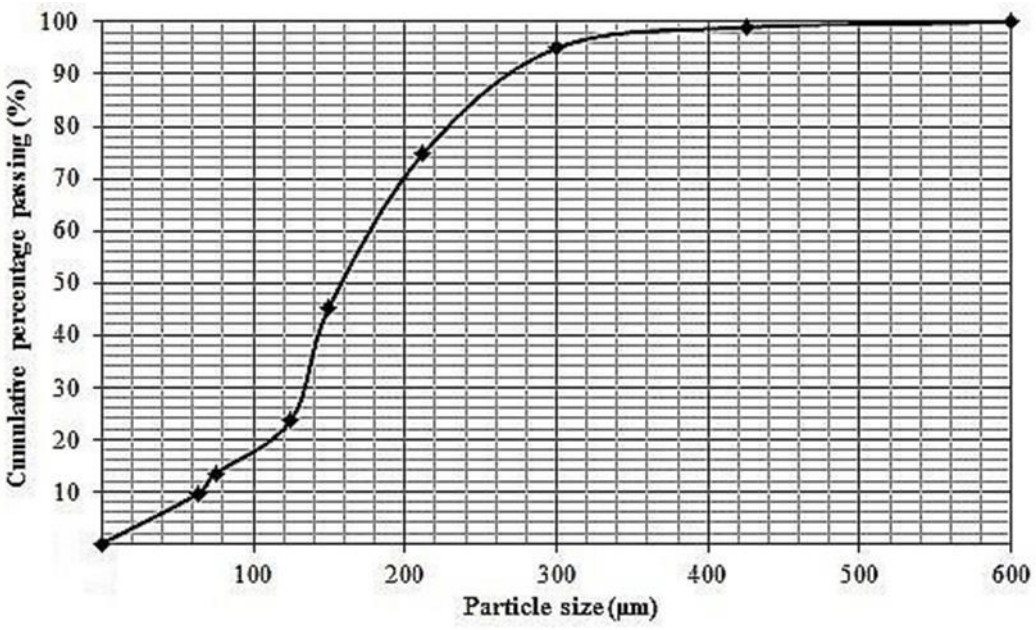

Fig.1. Particle size distribution of olivine

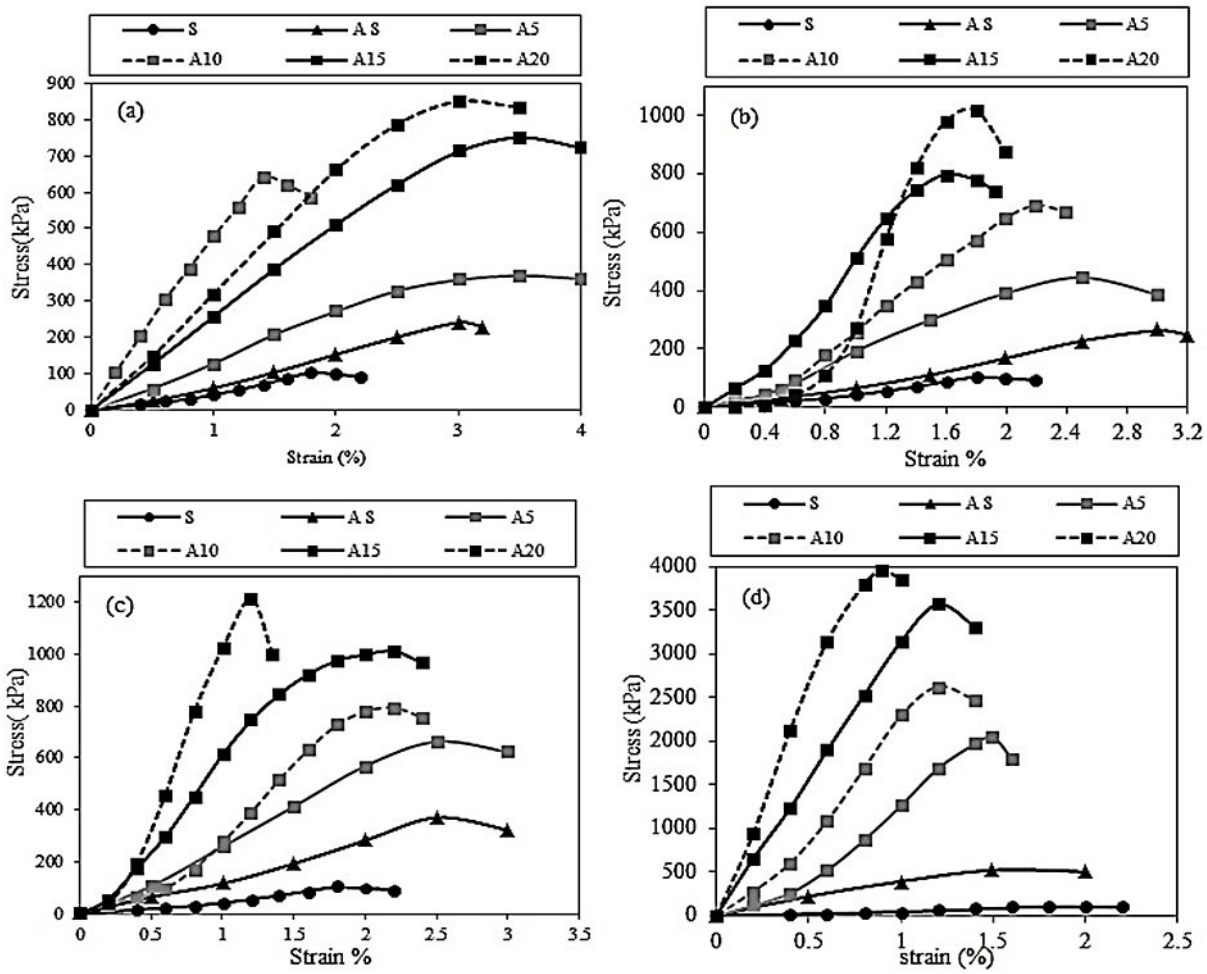

Fig.2. UCS of alkaline activated olivine treated soil at curing times of:
a) 7, b) 14, c) 28 and d) 90 days

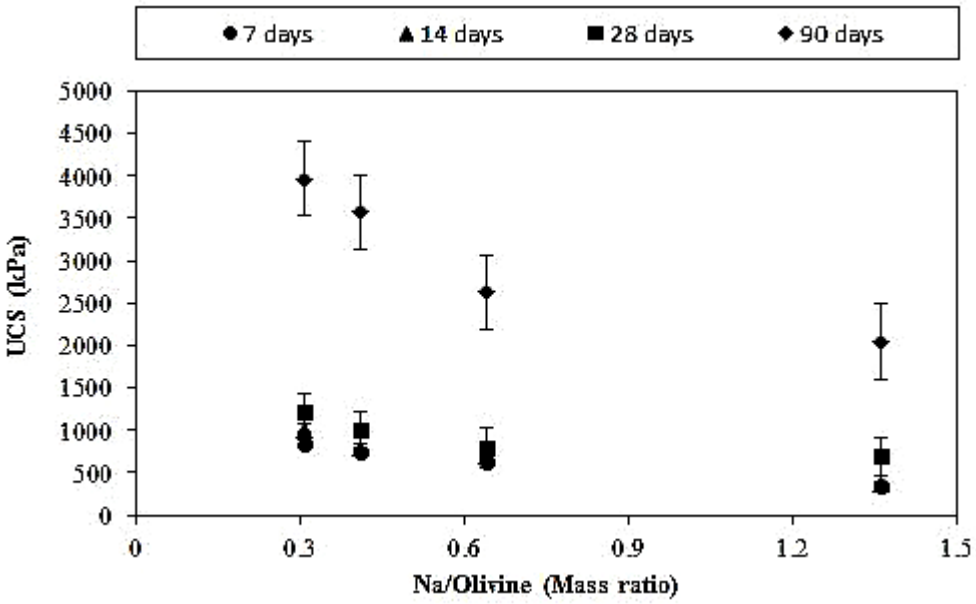

Fig.3. Influence of Na/olivine weight ratio on strength development at 7, 14, 28 and 90 days

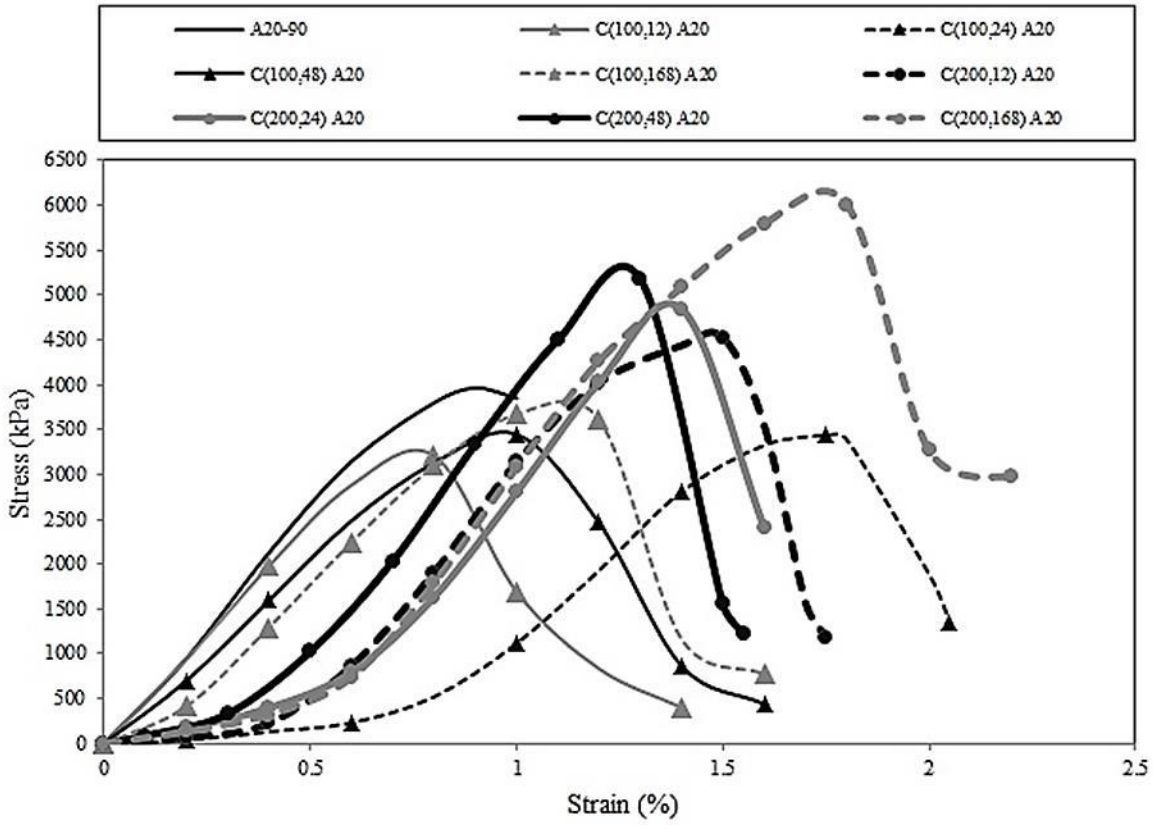

Fig.4. UCS of carbonated alkaline activated olivine treated soil subjected to carbonation for 12, 24, 48 and 168 hours at pressures of 100 and 200 kPa.

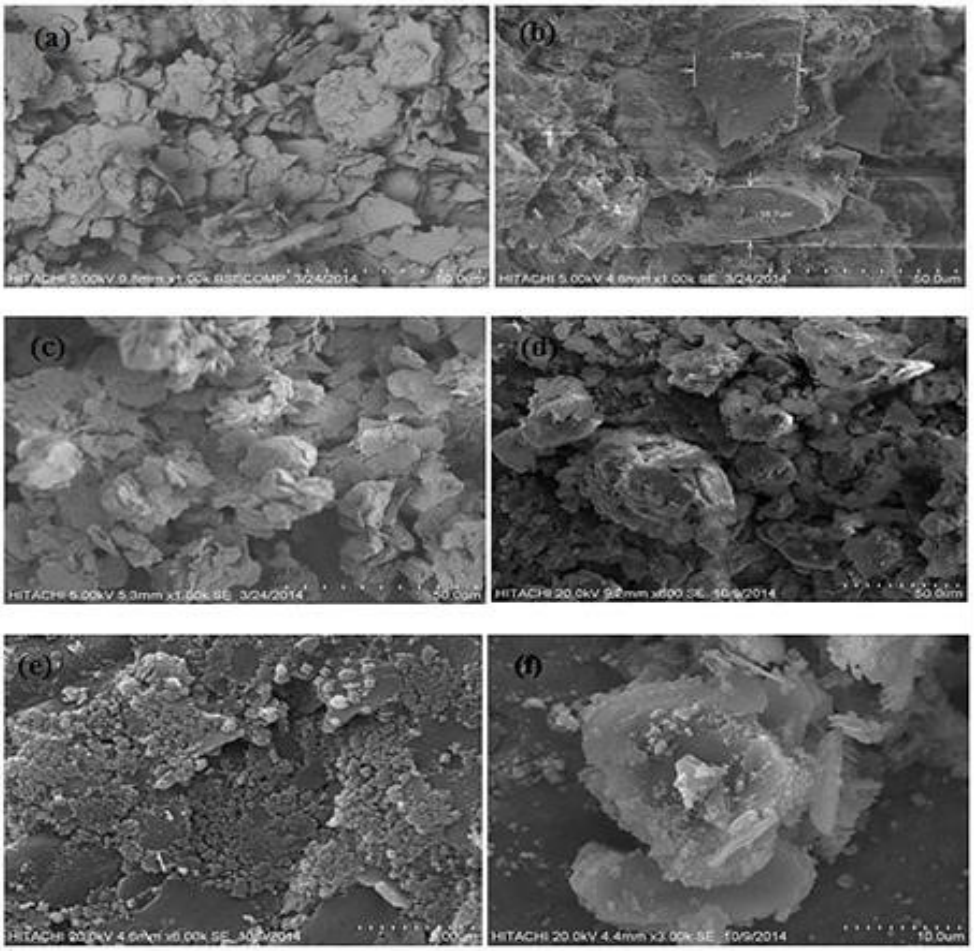

Fig.5. SEM images of: a) Soil, b) olivine, c) olivine treated soil and d-f) alkaline activated olivine treated soil after 90 days curing

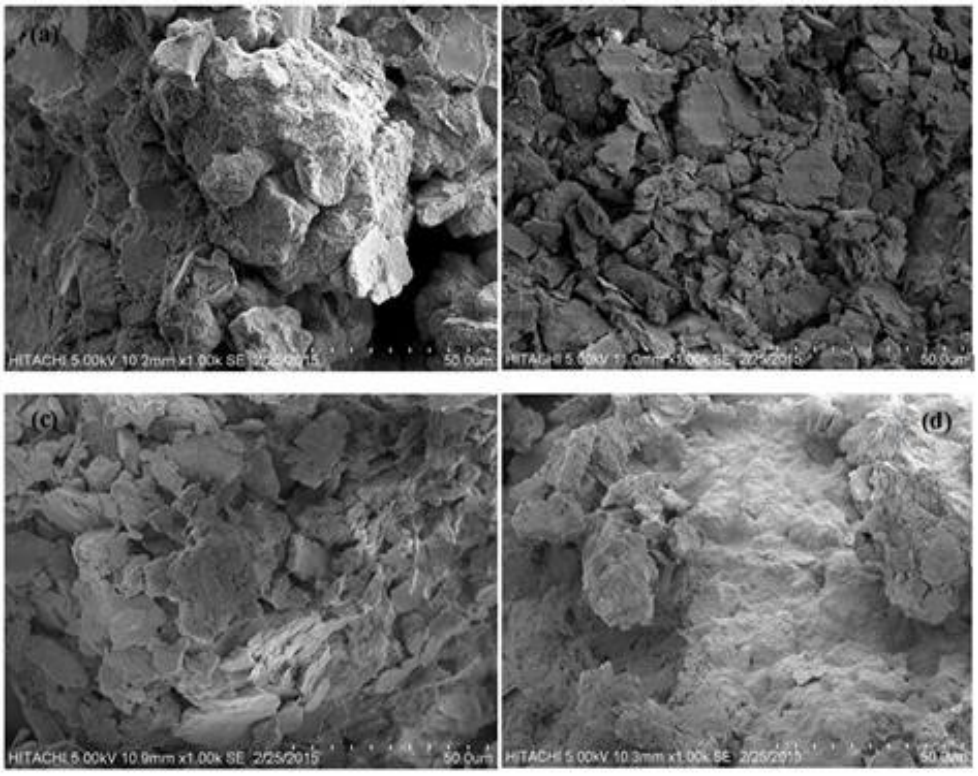

Fig.6. SEM images of: a) $C_{(200,12)}A20$, b)$C_{(200,24)}A20$, c) $C_{(200,48)}A20$ and d) $C_{(200,168)}A20$

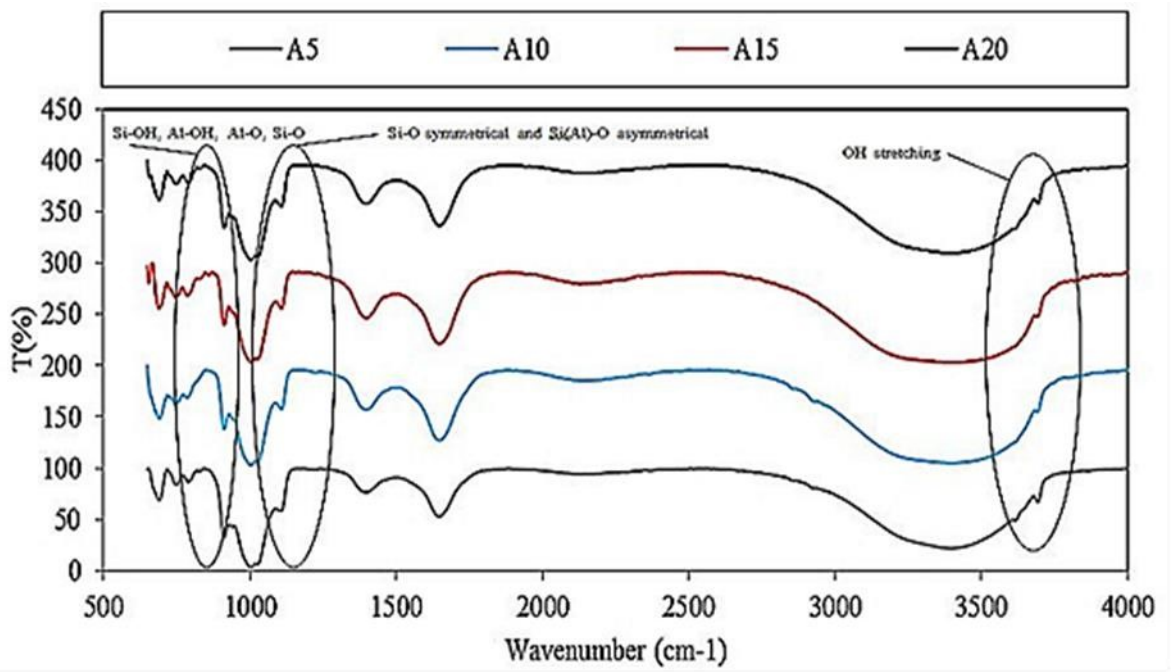

Fig.7. FTIR of alkaline activated olivine treated soil at different curing time

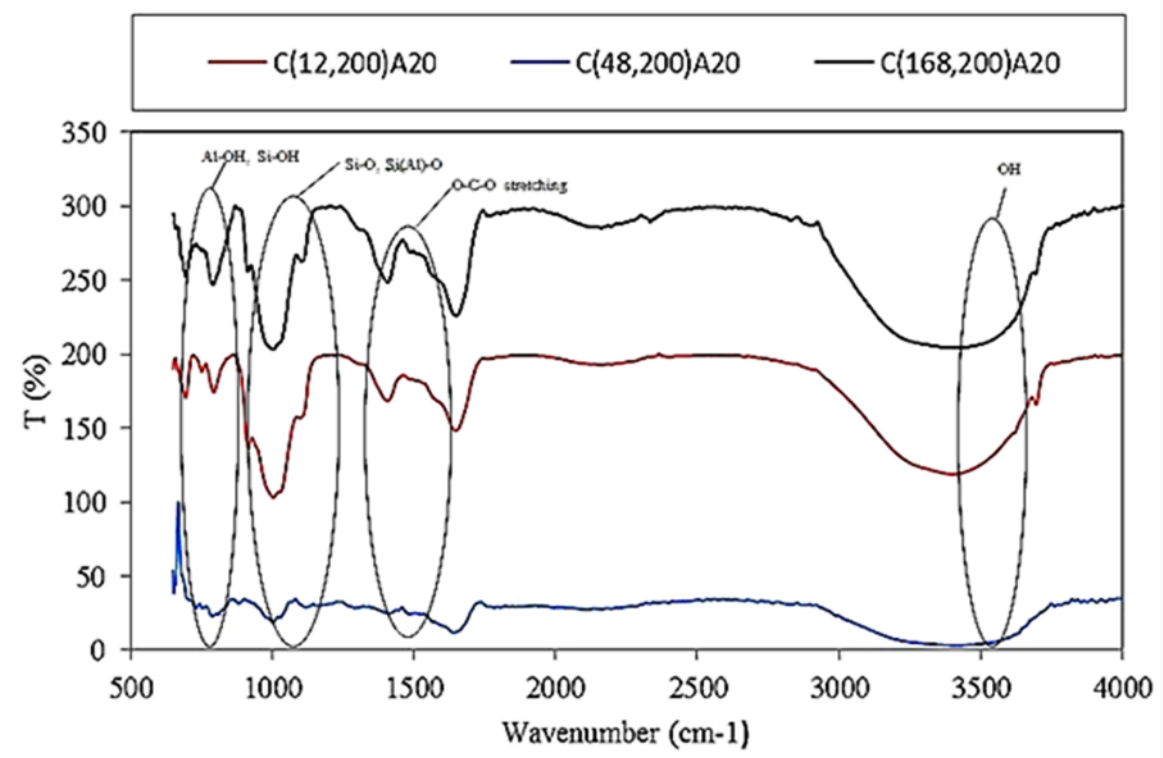

Fig.8. FTIR of carbonated alkaline activated olivine treated soil at 200 kPa pressure for 12, 48, 168 hours

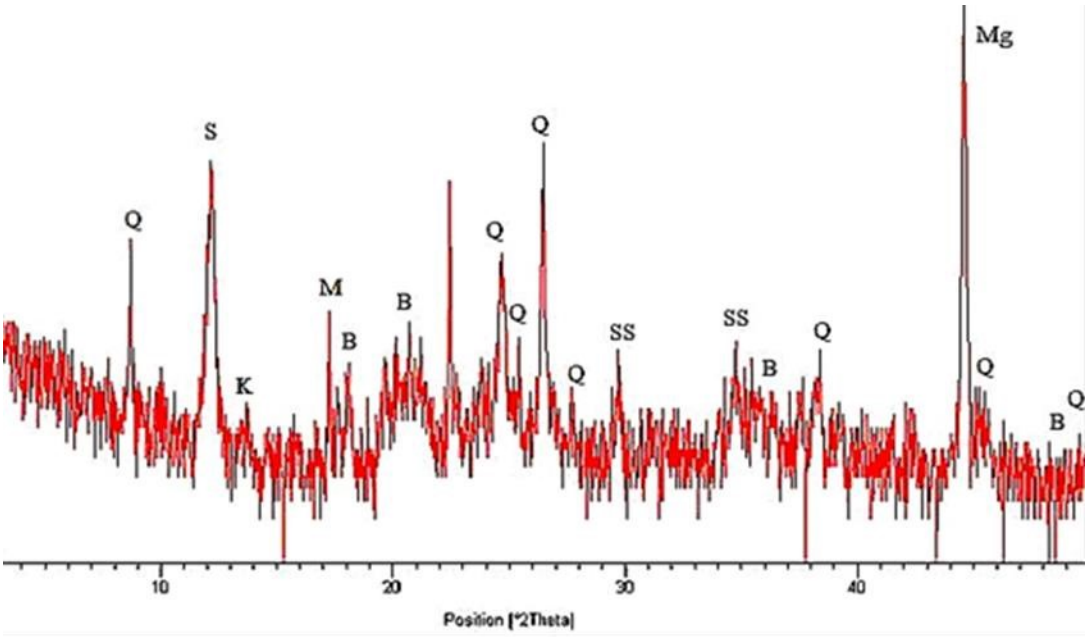

Fig.9. XRD of A20 after 90 days curing time (B:btucite, K:kaolinite, Mg:MgO, M:mullite, S:serpentine, SS:sodium silicate, Q:quartz)

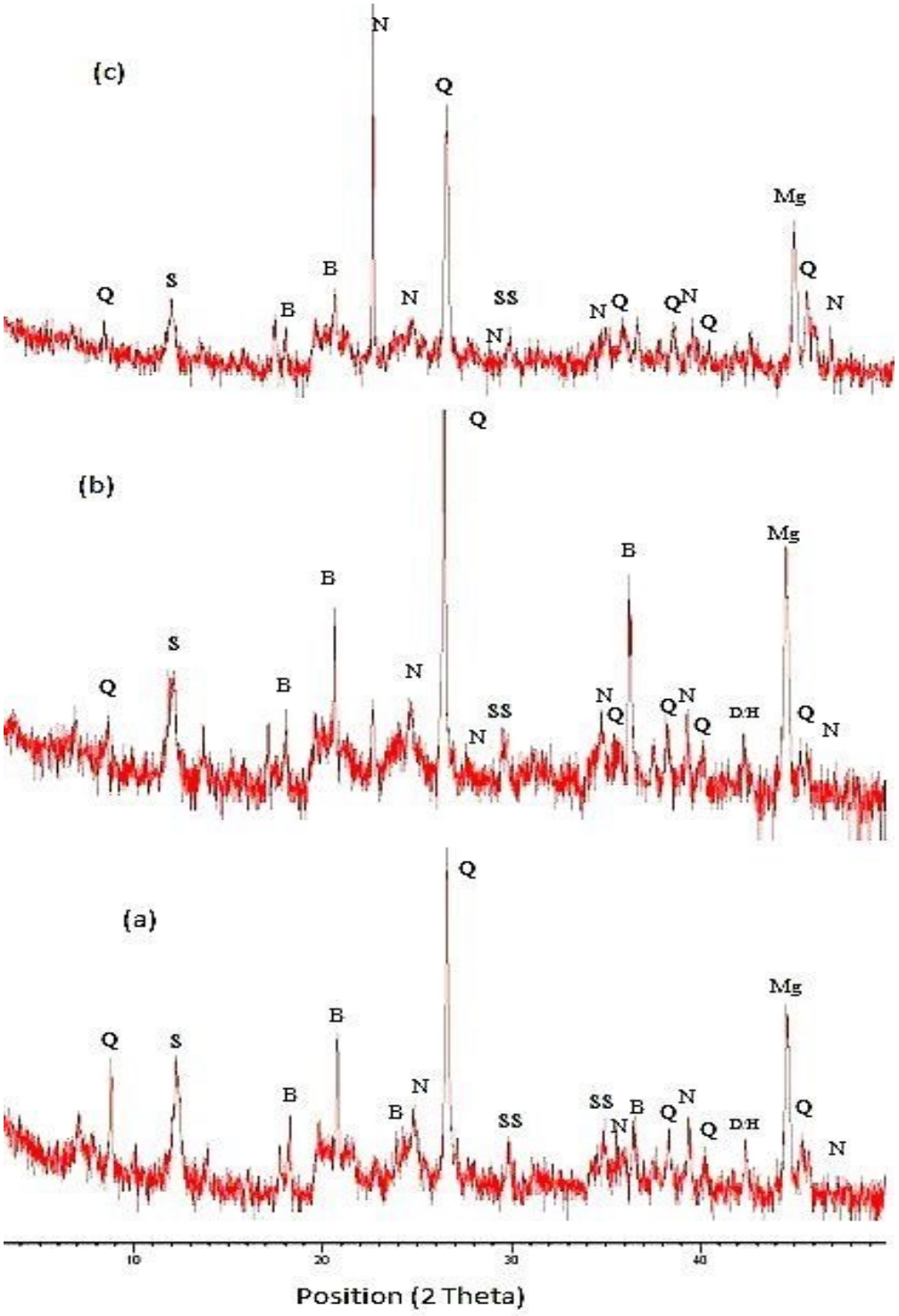

Fig.10. The XRD of: a) $C_{(12,200)}A_{20}$, b) $C_{(48,200)}A_{20}$ c) and $C_{(168,200)}A_{20}$ (B:brucite,H/D:hydromagnesite/dypingite, Mg:MgO, N:nesquehonite, Q:quartz, S:serpentine, SS:sodium silicate)

Figure Caption List

Fig.1. Particle size distribution of olivine

Fig.2. UCS of alkaline activated olivine treated soil at curing times of: a) 7, b) 14, c) 28 and d) 90 days

Fig.3. Influence of Na/olivine weight ratio on strength development at 7, 14, 28 and 90 days

Fig.4. UCS of carbonated alkaline activated olivine treated soil subjected to carbonation for 12, 24, 48 and 168 hours at pressures of 100 and 200 kPa.

Fig.5. SEM images of: a) Soil, b) olivine, c) olivine treated soil and d-f) alkaline activated olivine treated soil after 90 days curing

Fig.6. SEM images of: a) $C_{(200,12)}A20$, b)$C_{(200,24)}A20$, c) $C_{(200,48)}A20$ and d) $C_{(200,168)}A20$

Fig.7. FTIR of alkaline activated olivine treated soil at different curing time

Fig.8. FTIR of carbonated alkaline activated olivine treated soil at 200 kPa pressure for 12, 48, 168 hours

Fig.9. XRD of A20 after 90 days curing time (B:btucite, K:kaolinite, Mg:MgO, M:mullite, S:serpentine, SS:sodium silicate, Q:quartz)

Fig.10. The XRD of: a) $C_{(12,200)}A_{20}$, b) $C_{(48,200)}A_{20}$ c) and $C_{(168,200)}A_{20}$ (B:brucite, H/D:hydromagnesite/dypingite, Mg:MgO, N:nesquehonite, Q:quartz, S:serpentine, SS:sodium silicate)